Propagation and localization of acoustic waves in Fibonacci phononic circuits

2005 J. Phys.: Condens. Matter 17 4245

(http://iopscience.iop.org/0953-8984/17/27/002)

INSTITUTE OF PHYSICS PUBLISHING JOURNAL OF PHYSICS: CONDENSED MATTER

J. Phys.: Condens. Matter **17** (2005) 4245–4262 doi:10.1088/0953-8984/17/27/002

Propagation and localization of acoustic waves in Fibonacci phononic circuits

H Aynaou[1], E H El Boudouti[1], B Djafari-Rouhani[2], A Akjouj[2] and V R Velasco[3]

[1] Laboratoire de Dynamique et d'Optique des Matériaux, Département de Physique, Faculté des Sciences, Université Mohamed Premier, 60000 Oujda, Morocco
[2] Laboratoire de Dynamique et Structure des Matériaux Moléculaires, UMR CNRS 8024, UFR de Physique, Université de Lille 1, F-59655 Villeneuve d'Ascq, France
[3] Instituto de Ciencia de Materiales de Madrid, CSIC, Sor Juana Inés de la Cruz 3, 28049 Madrid, Spain

Received 29 March 2005, in final form 8 June 2005
Published 24 June 2005
Online at stacks.iop.org/JPhysCM/17/4245

Abstract

A theoretical investigation is made of acoustic wave propagation in one-dimensional phononic bandgap structures made of slender tube loops pasted together with slender tubes of finite length according to a Fibonacci sequence. The band structure and transmission spectrum is studied for two particular cases. (i) *Symmetric loop structures*, which are shown to be equivalent to diameter-modulated slender tubes. In this case, it is found that besides the existence of extended and forbidden modes, some narrow frequency bands appear in the transmission spectra inside the gaps as defect modes. The spatial localization of the modes lying in the middle of the bands and at their edges is examined by means of the local density of states. The dependence of the bandgap structure on the slender tube diameters is presented. An analysis of the transmission phase time enables us to derive the group velocity as well as the density of states in these structures. In particular, the stop bands (localized modes) may give rise to unusual (strong normal) dispersion in the gaps, yielding fast (slow) group velocities above (below) the speed of sound. (ii) *Asymmetric tube loop structures*, where the loops play the role of resonators that may introduce transmission zeros and hence new gaps unnoticed in the case of simple diameter-modulated slender tubes. The Fibonacci scaling property has been checked for both cases (i) and (ii), and it holds for a periodicity of three or six depending on the nature of the substrates surrounding the structure.

1. Introduction

There has been considerable recent interest in the propagation of classical waves—electromagnetic and acoustic—in periodically structured environments in analogy to electrons

in semiconductor crystals [1–4]. These materials, called photonic bandgap (PBG) and acoustic bandgap (ABG) crystals, allow the propagation of light, sound and vibration to be regulated. Each of these systems is composed of periodically modulated dielectric and elastic/acoustic media respectively. The propagation of acoustic waves in a so-called 'phononic crystal' was investigated theoretically [5] and experimentally [6] in two-dimensional (2D) and three-dimensional (3D) composite systems constituted by periodic inclusions of a given material in a host matrix. Such systems can exhibit an absolute ABG where the propagation of sound waves and ultrasonic vibrations is inhibited in any direction of the space. ABG materials can have many practical applications such as elastic/acoustic filters [7], ultrasonic silent blocks [8], acoustic mirrors, and improvement in the design of ultrasonic transducers using piezoelectric composites [9]. Studies of lower dimensional systems such as 1D periodic layered media [10, 11] and periodic waveguide systems with different geometries [12–20] are conducted as analogues of 2D and 3D systems and for applications in their own right. These structures are attractive since their production is more feasible at any wavelength scale and they require only simple analytical and numerical calculations. Besides periodic systems, quasi-regular ones with constituents arranged in quasi-periodic fashion have been intensively studied in the last years [21]. Since the pioneering work of Merlin *et al* [22] on non-periodic Fibonacci GaAs–AlAs superlattices, much attention has been paid to observe the exotic phenomena of Fibonacci systems [23, 24]. Interesting properties of these systems have been deduced [25, 26] mainly by theoretical studies based on simple 1D models. Another important motivation for studying these structures comes from recognizing that deterministic quasiperiodic systems may exhibit localization, such as the Anderson localization, of sound and vibration [27]. Such localization is a feature related to any wave when there exists disorder in the structures. It has been reported, for example, in acoustic waves [28–30] and optical waves [31]. However, the localization effect was not immediately apparent in the former case, whereas it was achieved in the latter one.

In a previous paper [14], some of the authors have studied the propagation of acoustic waves in 1D comb structures composed of dangling side branches periodically grafted at N equidistant sites on slender tubes. These theoretical results are confirmed by simple experiments using an impulse response technique [17], showing that it is possible via impulse reshaping to achieve group velocities more than twice the speed of sound. Similar experiments [18, 19] have been performed on periodically structured waveguides in the presence of a defect, showing the existence of slow group velocity of sound associated with the high dispersion in the vicinity of a narrow transmission band defect mode which could be of use in developing strong acoustic fields necessary for macrosonics applications. Recently [20], a different structure called a serial loop structure made of slender tubes pasted together periodically by asymmetric slender loops has been studied theoretically by some of the authors. In particular, it was demonstrated that these structures may present large gaps and are good candidates for ABG materials. The purpose of this paper is to give an extension of this work when the slender tube loops and the slender tubes are arranged in a quasi-periodic way. The quasiperiodic structures are generally known as substitutional sequences built of two different building blocks A and B. One of the best known examples is the Fibonacci sequence $S_{k+1} = S_k S_{k-1}$ with the initial conditions $S_1 = \mathrm{A}$, $S_2 = \mathrm{AB}$ where k is the generation number. For example $S_3 = \mathrm{ABA}$, $S_4 = \mathrm{ABAAB}$, $S_5 = \mathrm{ABAABABA}$, ... In this work, block A is made of a slender tube characterized by a length d_1 and a section a_1, whereas block B is made of a slender tube loop where the two arms of the ring have different lengths and sections, d_2 and a_2 (medium 2) and d_3 and section a_3 (medium 3). The finite structure is sandwiched between two slender tubes of sections a_s. We shall call it a *Fibonacci serial loop structure* (FSLS) (see for example figure 1 for the fifth generation structure).

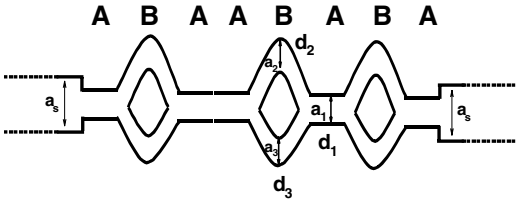

Figure 1. Schematic illustration of the 1D finite fifth Fibonacci structure made of A and B blocks. Block A is constructed from a slender tube of section a_1 and length d_1, whereas block B is a slender tube loop with two different arms of lengths d_2 and d_3 and sections a_2 and a_3 respectively. The finite structure is sandwiched between two slender tubes of sections a_s.

Motivated by the recent experimental works on periodic acoustic waveguides [13, 16–19], the specific emphasis in this work is twofold.

(i) In the case of symmetric FSLSs, we examine some transmission scaling properties of Fibonacci 1D structures depending on the nature of the substrates surrounding the finite structure. In addition, we show that besides the transmission amplitude an analysis of the phase time enables us to determine the density of states as well as the group velocity in these structures.

(ii) In the case of asymmetric FSLSs, we show that besides the gaps present in symmetric FSLSs, some new gaps appear in the band structures as the consequence of the transmission zeros induced by asymmetric loops which play the role of resonators. The Fibonacci scaling property has been shown to be also present in the case of asymmetric loops.

The rest of the paper is organized as follows: in section 2 we give a brief presentation of the method of calculation employed here, which is based on the Green function method. Section 3 is devoted to the discussion of the numerical results for symmetric and asymmetric FSLSs with different geometries. The final section contains the concluding remarks.

2. Method of theoretical and numerical calculation

2.1. Interface response theory of continuous media

Our theoretical analysis is performed with the help of the interface response theory of continuous media, which allows calculation of the Green function of any composite material. In what follows, we present the basic concept and the fundamental equations of this theory [32]. Let us consider any composite material contained in its space of definition D and formed out of N different homogeneous pieces located in their domains D_i. Each piece is bounded by an interface M_i, adjacent in general to j $(1 \leqslant j \leqslant J)$ other pieces through subinterface domains M_{ij}. The ensemble of all these interface spaces M_i will be called the interface space M of the composite material. The elements of the Green function $g(DD)$ of any composite material can be obtained from [32]

$$g(DD) = G(DD) - G(DM)G^{-1}(MM)G(MD) + G(DM)G^{-1}(MM)g(MM)G^{-1}(MM)G(MD), \quad (1)$$

where $G(DD)$ is the reference Green function formed out of truncated pieces in D_i of the bulk Green functions of the infinite continuous media and $g(MM)$, the interface element of the Green function of the composite system. The inverse of $g(MM)$ is obtained as a superposition of the different $[g_i(M_i, M_i)]^{-1}$, where $g_i(M_i, M_i)$ is the interface Green function for each

constituent i of the composite system [32]. The knowledge of the inverse of $g(MM)$ is sufficient to calculate the interface states of a composite system through the relation [32]

$$\det[g^{-1}(MM)] = 0. \tag{2}$$

Moreover if $U(D)$ represents an eigenvector of the reference system, equation (1) enables the calculation of the eigenvectors $u(D)$ of the composite material

$$u(D) = U(D) - U(M)G^{-1}(MM)G(MD) + U(M)G^{-1}(MM)g(MM)G^{-1}(MM)G(MD). \tag{3}$$

ln equation (3), $U(D)$, $U(M)$, and $u(D)$ are row vectors. Equation (3) provides a description of all the waves reflected and transmitted by the interfaces, as well as the reflection and transmission coefficients of the composite system. ln this case, $U(D)$ is a bulk wave launched from one of the substrate media [33].

2.2. *Inverse surface Green functions of the elementary constituents*

We consider an infinite homogeneous isotropic slender tube i characterized by its characteristic impedance $Z_i = \rho_i v_0/a_i$ where ρ_i is the mass density, a_i the cross-section and v_0 the longitudinal speed of sound. The Fourier transformed Green function between two points x and x' of this slender tube is

$$G_i(x, x') = \tfrac{1}{2}\mathrm{j}Z_i\mathrm{e}^{-\alpha_i|x-x'|}, \tag{4}$$

with

$$\alpha_i = \mathrm{j}\frac{\omega}{v_0}, \tag{5}$$

ω being the angular frequency of the wave and $\mathrm{j} = \sqrt{-1}$.

Before addressing the problem of the FSLS, it is helpful to know the surface elements of its elementary constituents, namely, the Green function of a finite slender tube of length d_1, of a loop made of two tubes 2 and 3 of lengths d_2 and d_3 respectively, and of a semi-infinite tube s. The finite slender tube is bounded by two free surfaces located at $x = -\frac{d_1}{2}$ and $+\frac{d_1}{2}$. These surface elements can be written in the form of a (2×2) matrix $g_1(MM)$, within the interface space $M_1 = \{-\frac{d_1}{2}, +\frac{d_1}{2}\}$. The inverse of this matrix takes the following form [33]:

$$[g_1(MM)]^{-1} = \begin{pmatrix} \frac{C_1}{Z_1 S_1'} & -\frac{1}{Z_1 S_1'} \\ -\frac{1}{Z_1 S_1'} & \frac{C_1}{Z_1 S_1'} \end{pmatrix}. \tag{6}$$

In the same way, the inverse of the Green function of the loop (2), (3) is obtained as

$$[g_{2,3}(MM)]^{-1} = \begin{pmatrix} \frac{C_2}{Z_2 S_2'} + \frac{C_3}{Z_3 S_3'} & -\frac{1}{Z_2 S_2'} - \frac{1}{Z_3 S_3'} \\ -\frac{1}{Z_2 S_2'} - \frac{1}{Z_3 S_3'} & \frac{C_2}{Z_2 S_2'} + \frac{C_3}{Z_3 S_3'} \end{pmatrix}, \tag{7}$$

where $C_i = \cos(\omega_i d_i/v_0)$ and $S_i' = \sin(\omega_i d_i/v_0)$ in equations (6) and (7) $(i = 1, 2, 3)$. The inverse of the surface element of a semi-infinite tube s characterized by its impedance $Z_s = \rho_s v_0/a_s$ is given by

$$[g_s(0, 0)]^{-1} = -\frac{\mathrm{j}}{Z_s}. \tag{8}$$

From equation (7) one can deduce that a symmetric loop made of identical tubes of lengths $d_2 = d_3$ and impedances $Z_2 = Z_3$ (i.e., $a_2 = a_3$) is equivalent to a single segment of length d_2 and characterized by the impedance $Z_2/2 = \rho_2 v_0/2a_2$ (i.e., a simple slender tube with a

double cross-section). Therefore, the structure of figure 1 becomes equivalent to a diameter-modulated waveguide array. The experimental evidence of the existence of bandgaps and defect modes in 1D periodic acoustic systems constructed by two alternative slender tubes of different cross-sections was presented recently [18, 19]. However, the advantage of the symmetric loop structure lies in the fact that it is not necessary to have two segments of different natures to realize the contrast between the two constituent media of each block. This property could be of potential interest in acoustical waveguide structures. It should be pointed out that the validity of our results is subject to the requirement $\sqrt{a_i} \ll d_i, \lambda$, i.e., the cross section of the slender tubes being negligible compared to their length and to the propagation wavelength λ. The assumption of monomode propagation is then satisfied.

2.3. Transmission coefficient

The 1D FSLS waveguide can be considered as a finite number of blocks A and B pasted together according to the Fibonacci sequence. The interface domain is made of all the connection points between finite tubes and tube loops. Within the total interface space of the finite FSLS, the inverse of the matrix giving all the interface elements of the Green function g is a finite tridiagonal matrix formed by the linear superposition of the elements $[g_i(MM)]^{-1}$ (equations (6) and (7)). The explicit expression of the Green function elements of the finite FSLS may be written as

$$g_f^{-1}(MM) = \begin{pmatrix} g_f^{-1}(\ell,\ell) & g_f^{-1}(\ell,r) \\ g_f^{-1}(r,\ell) & g_f^{-1}(r,r) \end{pmatrix} \tag{9}$$

where the labels ℓ (left) and r (right) refer to the two interfaces bounding the FSLS. The four matrix elements are real quantities, functions of the different elements of the constituent's elements $g_i(MM)$ (equations (6) and (7)). If the finite composite system is sandwiched between two homogeneous waveguides labelled s, then an incident plane wave launched from the left waveguide gives rise to the transmission function in the right waveguide as

$$C_T = \frac{\mathrm{j}2g_f^{-1}(l,r)/Z_s}{g_f^{-1}(\ell,\ell)g_f^{-1}(r,r) - [g_f^{-1}(l,r)]^2 - (1/Z_s)^2 - \mathrm{j}(g_f^{-1}(\ell,\ell) + g_f^{-1}(r,r))/Z_s}. \tag{10}$$

The transmission function can be written in an explicit complex form as $C_T = a + \mathrm{j}b = \sqrt{T}\mathrm{e}^{\mathrm{j}\varphi}$ where T is the transmission coefficient, $\varphi = \arctan(b/a) \pm m\pi$ is the phase associated with the transmission field and m is an integer. The first derivative of φ with respect to the frequency is related to the delay time taken by the wave to traverse the structure. This quantity, called the phase time, is defined by [34, 35]

$$\tau_\varphi = \frac{\mathrm{d}\varphi}{\mathrm{d}\omega}. \tag{11}$$

From equations (10) and (11), one can deduce that the phase time can be written as

$$\tau_\varphi = \frac{\mathrm{d}}{\mathrm{d}\omega}\arg[g_f^{-1}(\ell,\ell)g_f^{-1}(r,r) - (g_f^{-1}(\ell,r))^2 - (1/Z_s)^2 - \mathrm{j}(g_f^{-1}(\ell,\ell) + g_f^{-1}(r,r))/Z_s]^{-1} + \frac{\mathrm{d}}{\mathrm{d}\omega}\arg[g_f^{-1}(\ell,r)]. \tag{12}$$

Furthermore, the DOS of the present composite system from which we have subtracted the DOS of the same volumes of the semi-infinite tubes s is given by [32, 35]

$$\Delta n(\omega) = \frac{1}{\pi}\frac{\mathrm{d}}{\mathrm{d}\omega}\arg[g_f^{-1}(\ell,\ell)g_f^{-1}(r,r) - (g_f^{-1}(\ell,r))^2 - (1/Z_s)^2 - \mathrm{j}(g_f^{-1}(\ell,\ell) + g_f^{-1}(r,r))/Z_s]^{-1}. \tag{13}$$

From equations (12) and (13) one can deduce two cases, namely, the following.

(i) The case of symmetrical loop structures that do not present transmission zeros (i.e., $g_f^{-1}(\ell, r) \neq 0$ in equation (10)). Then $\arg(g_f^{-1}(\ell, r)) = 0$ and $\tau_\varphi = \pi \Delta_n(\omega)$.

(ii) The case of asymmetrical loop structures, where transmission zeros occur at some frequencies we denote by ω_n (i.e., $g_f^{-1}(\ell, r) = 0$ in equation (10), $n = 1, 2, \ldots$). Then the transmission coefficient changes sign at ω_n and its phase exhibits a jump of π. In other words, the second term at the right-hand side of equation (12) becomes [36]

$$\frac{\mathrm{d}}{\mathrm{d}\omega}\arg(g_f^{-1}(\ell, r)) = \pi \sum_n \mathrm{sgn}\left[\frac{\mathrm{d}}{\mathrm{d}\omega}(g_f^{-1}(\ell, r))_{\omega=\omega_n}\right]\delta(\omega - \omega_n) \tag{14}$$

where sgn means the sign function. This result means that $\tau_\varphi \neq \pi \Delta_n(\omega)$ as τ_φ (equation (12)) may exhibit δ functions at the transmission zeros that do not exist in the variation of the DOS (equation (13)). Both cases (i) and (ii) will be illustrated below in relation to symmetric and asymmetric FSLSs respectively.

3. Illustrative examples

We focus in this paper on homogeneous FSLSs where the tubes are filled with the same fluid but have different lengths and cross sections. In addition, we shall emphasize two particular cases depending on the lengths of the arms constituting the slender loops.

(i) The case where the loops in each block are symmetrical and identical (i.e., $d_2 = d_3$ and $a_2 = a_3$). As mentioned above, the symmetric loop becomes equivalent to a simple slender tube with $d_\mathrm{B} = d_2 = d_3$ and $a_\mathrm{B} = 2a_2$ in block B. We shall also call $d_1 = d_\mathrm{A}$ and $a_1 = a_\mathrm{A}$ in the slender tube of block A.

(ii) The case where the tubes constituting the two arms of the loop are supposed to be filled with the same fluid but with different lengths (i.e., $a_2 = a_3$ and $d_2 \neq d_3$ but keeping the total length of the loop $d_2 + d_3$ unchanged).

3.1. Case of symmetric FSLS

As mentioned above, the FSLS (figure 1) becomes equivalent to a diameter-modulated waveguide constituted by two slender tubes A and B characterized by their lengths $d_\mathrm{A} = d_1$ and $d_\mathrm{B} = d_2$ and their cross-sections $a_\mathrm{A} = a_1$ and $a_\mathrm{B} = 2a_2$ respectively. Figures 2(b)–(f) show the transmission coefficient as a function of the reduced frequency $\Omega = \omega d_1/v_0$ for the Fibonacci generations S_5 (8 blocks), S_6 (13 blocks), S_7 (21 blocks), S_8 (34 blocks) and S_9 (55 blocks) respectively. The finite FSLS is sandwiched between two media of material of type A (i.e., $a_s = a_\mathrm{A}$). Due to the finiteness of the systems the importance of the boundary conditions (the media limiting the structure) cannot be ignored. Thus we shall see at the end of this section that different results are obtained when the surrounding media are of type B (i.e., $a_s = a_\mathrm{B}$). Two regions of frequencies may be distinguished in figures 2(b)–(e): the regions where the transmission falls rapidly to zero as the generation number increases (these regions correspond to the forbidden modes, pseudo-bandgaps) and the regions where the transmission is more noticeable around $\Omega = 0,\ \pi,\ 2\pi, \ldots$ (these regions correspond to the allowed modes, pseudo-bands). In the middle of the gaps around $\pi/2, 3\pi/2, \ldots$ some peaks appear as defect modes. The number of these modes increases as a function of the generation number. As a matter of comparison, we have also given the transmission spectrum of the periodic structure (figure 2(a)) where the stop bands do not show, as expected, any new features. These results

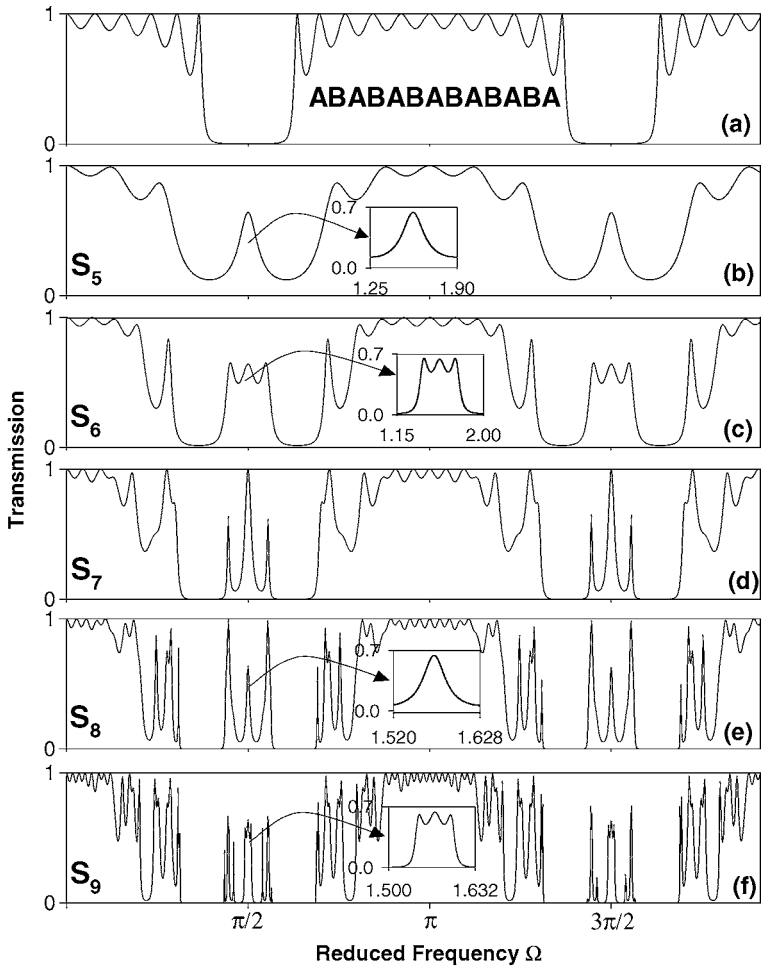

Figure 2. The variation of the transmission coefficient as a function of the reduced frequency $\Omega = \omega d_1/v_0$ for (a) the periodic structure and (b)–(f) different generations S_k ($k = 5$–9) of the Fibonacci loop structure respectively. The lengths of the different tubes are such that $d_1 = d_2 = d_3$ and $a_1 = a_2 = a_3$. The sections of the two media surrounding the structure are such that $a_s = a_1$.

show that the FSLSs present similar features as the periodic structure, but with new ones inside the gaps. These resonances present a certain recursive order which is a characteristic of Fibonacci systems. This property, called the scaling relation [37], has been interpreted as a sign of localization of the waves in Fibonacci systems. Kohmoto *et al* [37] have shown the existence of an invariant I which remains constant at every step of the recursive procedure, its expression being given by [37]

$$I = \frac{1}{4}\left(\frac{Z_A}{Z_B} - \frac{Z_B}{Z_A}\right)^2 \sin^2(\omega d_A/v_0)\sin^2(\omega d_B/v_0), \tag{15}$$

where $Z_A = \rho_A v_0/a_A$ and $Z_B = \rho_B v_0/a_B$ are the impedances of the two slender tubes constituting the FSLS. Also, it has been demonstrated [37] that one can expect scaling around $\delta = \omega d_A/v_0 = \omega d_B/v_0 = (2m + 1)\pi/2$ where the quasiperiodicity is most effective (m is an integer). This implies that the transmission coefficient should exhibit a self-similar

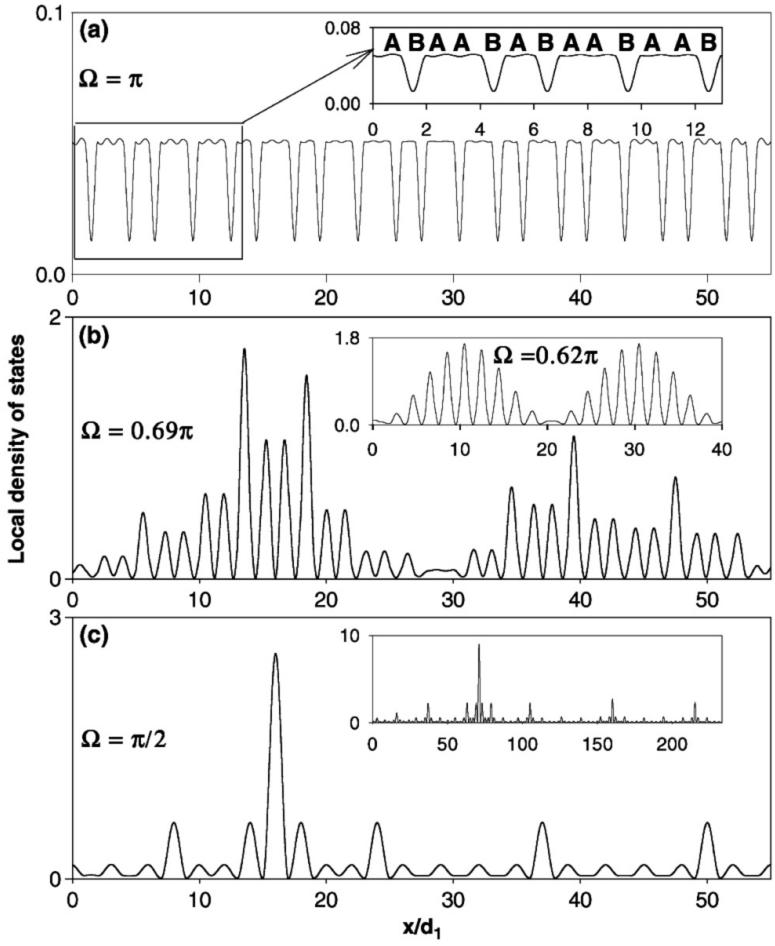

Figure 3. The local density of states (in arbitrary units) as a function of the space position x/d_1 for three frequencies belonging to figure 2(f): (a) $\Omega = \pi$ (middle of the band), (b) $\Omega = 0.69\pi$ (band edge), and (c) $\Omega = 0.5\pi$ (central frequency). The inset of (b) corresponds to the LDOS associated with the periodic structure at $\Omega = 0.62\pi$. The inset of (c) corresponds to the LDOS associated with the 12th generation at $\Omega = 0.5\pi$.

behaviour around the central frequency $\Omega_c = (2m + 1)\pi/2$ with $T_{j+3} = T_j$ (the period of the transmission coefficient is three recursions). The scale behaviour of the transmission coefficient is characterized by the scale factor [37]

$$f = \sqrt{1 + 4(1 + I)^2} + 2(1 + I). \tag{16}$$

For the central frequency $\Omega_c = (2m + 1)\pi/2$, I is maximum, i.e. $I = 0.526$ and thus $f = 6.4061$. The self-similarity of the transmission amplitude is clearly shown around Ω_c in the insets of figures 2(b) and (e) for the S_5 and S_8 generations and figures 2(c) and (f) for the S_6 and S_9 generations respectively. Note the scale change of the frequency axis for spectra S_8 and S_9 as compared to S_5 and S_6 respectively. These results are analogous to those found by Gellermann *et al* [31] on dielectric Fibonacci multilayers.

It is well established that outside the Fibonacci bandgaps the waves are critically localized [38]. In contrast with the fully disordered (Anderson) localized case, these critically localized modes decay more weakly than exponentially, most likely by a power law, and have

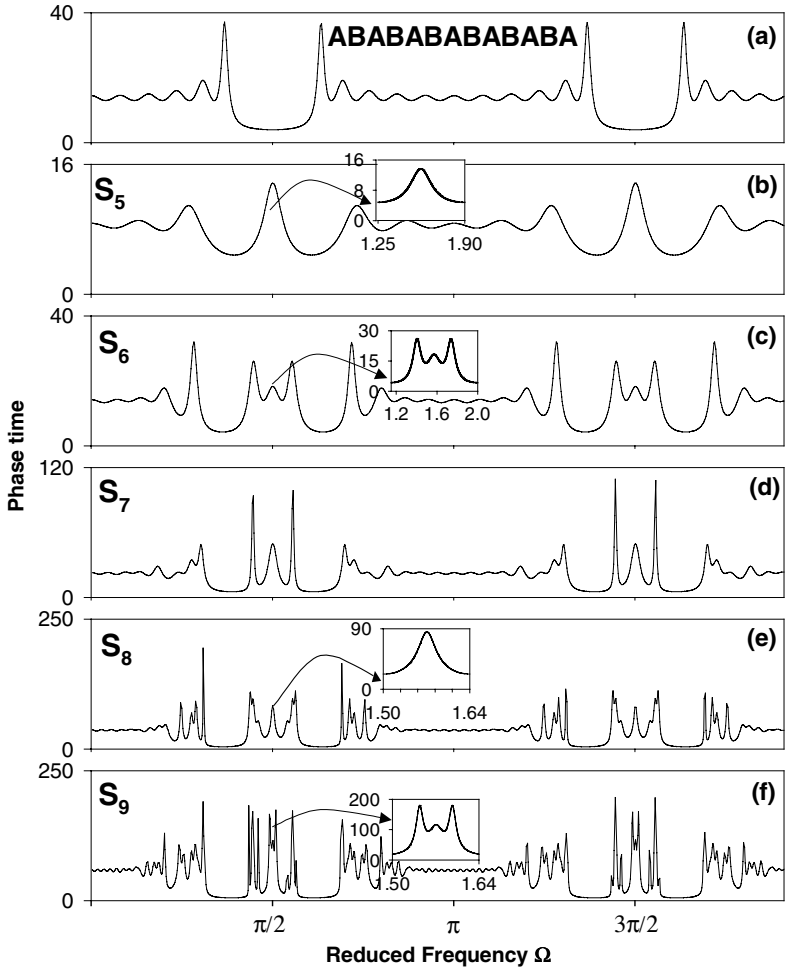

Figure 4. Phase time as a function of the reduced frequency. The other parameters are those of figure 2.

a rich self-similar structure [39]. In order to understand the spatial localization of the different modes in figure 2, we plot in figure 3 the LDOS as a function of the space position x for the modes lying at $\Omega = \pi$, 0.69π, and 0.5π in figure 2(f) (ninth generation). The LDOS reflects the square modulus of the pressure field inside the structure. These modes could be classified respectively as the following.

(i) Extended modes as shown in figure 3(a) for the completely transparent mode ($\Omega = \pi$) for which the transmission is unity [38]. The wavefunction, namely the pressure field distribution, follows the structure of the Fibonacci sequence (see the inset of figure 3(a)). This pressure distribution is analogous to the lattice-like wavefunction in the electronic problem [40] and the electric field in the electromagnetic problem [41].

(ii) Band-edge modes as shown in figure 3(b) for the mode $\Omega = 0.69\pi$. The LDOS shows (figure 3(b)) a noticeable similarity to the band edge resonances occurring in the periodic structure (see the inset of figure 3(b)) but is less regular. Band edge resonances in photonic periodic crystals are shown not to be localized states since their extension scales linearly

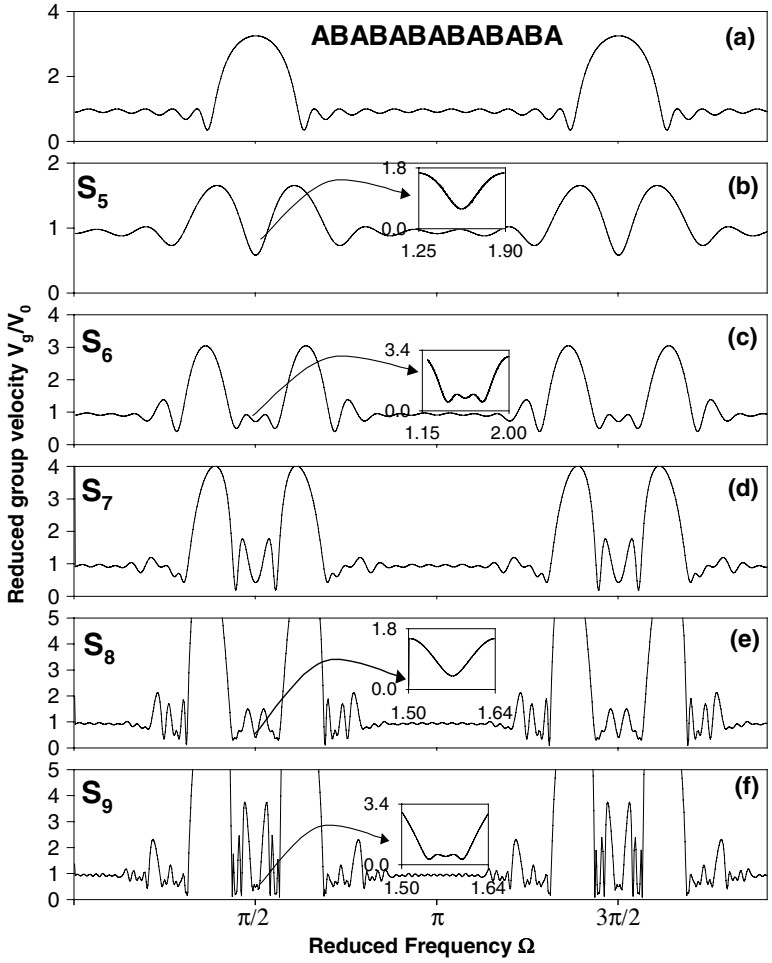

Figure 5. The same as figure 4 but for the group velocity.

with the system size and they do not decay to zero [42, 43]. In contrast, the Fibonacci band edge resonances will decay via a power law due to the Fibonacci disorder [44].

(iii) Self-similar modes as shown in figure 3(c) for the mode lying at $\Omega = 0.5\pi$. The corresponding LDOS shows a self-similar behaviour [42, 45] around the main peak every three generations (see the inset of figure 3(c) displayed for the 12th generation).

Another important quantity that characterizes the interaction of the incident phonon with the different modes in the FSLS is the transmission phase time. This quantity is interpreted as the time needed for a phonon to complete the transmission process. Figure 4 gives the phase time as a function of the reduced frequency Ω for the same structures as in figure 2. Apart from the bandgap edges, the modes lying inside the gaps give rise to large phase time in comparison with the modes lying inside the bulk bands. One can also notice that the phase time shows the same self-similarities (three recursions) as the transmission amplitude around the central frequency Ω_c. This is illustrated in the insets of figure 4 although the intensities of the peaks are not similar. As demonstrated in section 2.3, the phase time is equivalent to the density of states in these 1D phononic crystals which do not exhibit transmission zeros [30, 33]. From the

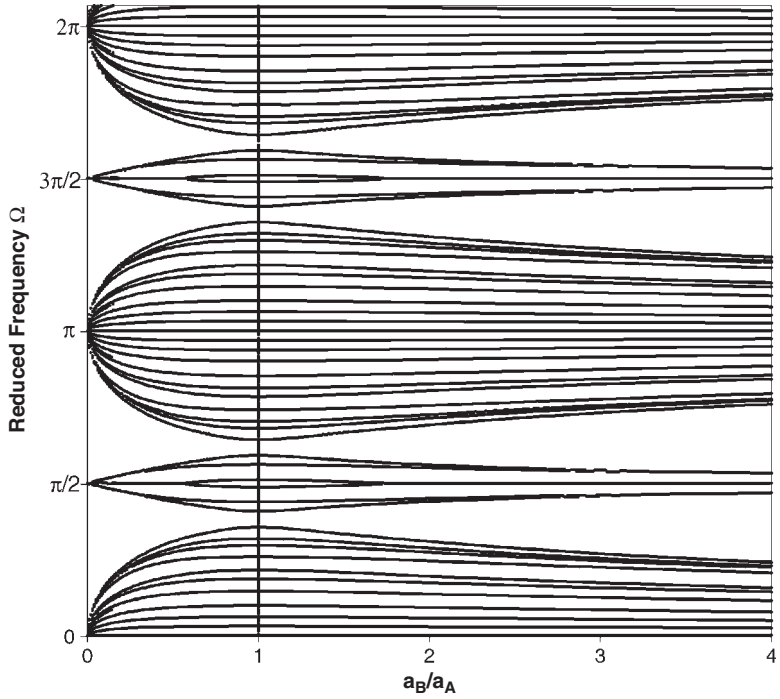

Figure 6. Projected band structure (reduced frequency Ω as a function of the cross-section ratio a_B/a_A) of the eighth Fibonacci generation. The other parameters are the same as in figure 2. The dots are obtained from the maxima of the phase time.

phase time one can also deduce the group velocity $v_g = L/\tau_\varphi$ [46], where L is the total length of the structure, i.e., the sum of the lengths of the A and B blocks constituting the structure (see figure 3). The existence of localized waves in FSLSs may be used as a tool to reduce the propagation speed of waves in such structures. Indeed, as argued recently [18, 19], the presence of a single defect in an otherwise periodic system made of two alternating different slender tubes may considerably reduce the group velocity in a narrow frequency band below the normal propagation speed in the tubes. Now, by introducing more than one defect in these structures as in Fibonacci systems, one can obtain a narrow frequency band where the velocity may be slower. These results are illustrated in figures 5(b)–(f), where we have plotted the group velocity v_g versus the frequency for the same structures as in figures 2 and 4. In the case of periodic structures (figure 5(a)), an anomalous dispersion occurs inside the gaps and velocities greater than the speed of sound are expected [17–19]. This result still remains for the Fibonacci quasi-periodic structures, although a small group velocity ($v_g \approx 0.2v_0$) lower than the normal speed of sound in the tubes (figures 5(b)–(f)) is obtained around the central frequencies. This value is the same as the one found experimentally by Robertson *et al* [19] in diameter-modulated waveguides. The group velocity clearly shows a self-similarity around the central frequency Ω_c as shown in the insets of figure 5. The slower group velocity may be explained by the time spent by the phonon (trapping time) inside some regions of the quasi-periodic structure (see figure 3(c)) before its transmission [44, 46]. Another interesting result in figures 4 and 5 concerns the behaviour of the phase time and the group velocity near the bandgap edges. Indeed, it is well known that in infinite 1D periodic systems the density of modes approaches infinity at the band edge and the group velocity becomes very small. In

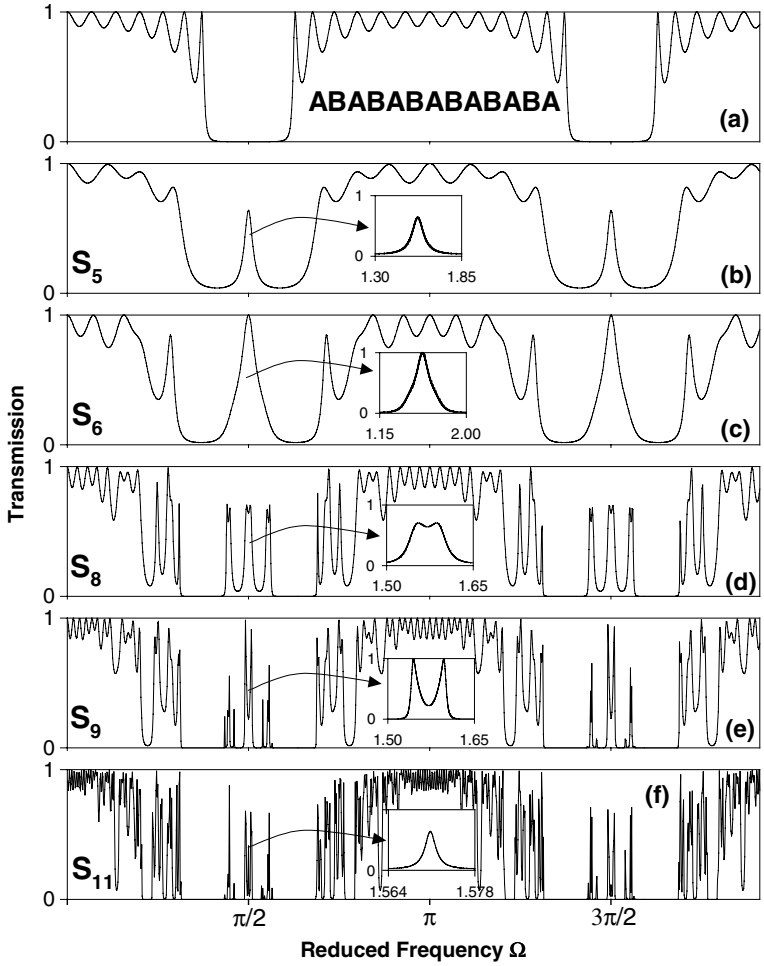

Figure 7. The same as figure 2 but the two media surrounding the structure are such that $a_s = a_B$.

a finite system, however, the acoustic mode density is an oscillating function rather than a monotonic function (figure 4(a)). The enhancement of the phase time (density of states) at the band edges induces a small group velocity ($v_g \approx 0.2v_0$) (figure 5). Inside the pass-bands, the group velocity is equal to v_0, which is the normal speed of wave propagation in the tubes.

In order to show the effect of the ratio of the cross-sections of the B and A blocks, we plotted in figure 6 the dispersion curves (the frequency Ω as a function of a_B/a_A or equivalently Z_A/Z_B) for the eighth generation. These frequencies (dots) are obtained from the maxima of the phase time (density of states). Figure 6 clearly shows that the bulk modes are strongly dependent upon a_B/a_A. When $a_B = a_A$ (i.e., $Z_A = Z_B$) the transmission is unity and the stop bands close. For $a_B \neq a_A$ the gap widths increase, giving rise to large gaps for small and big values of a_B/a_A, and also the narrow bands associated with localized modes inside the gaps become thinner. As mentioned at the beginning of this section, the results obtained above depend strongly on the nature of the media surrounding the finite FSLS. Indeed, when these media are of type B instead of A (i.e., $a_s = a_B$), figures 7 (transmission) and 8 (phase time) clearly show noticeable differences as compared to figures 2 and 4 respectively. In particular,

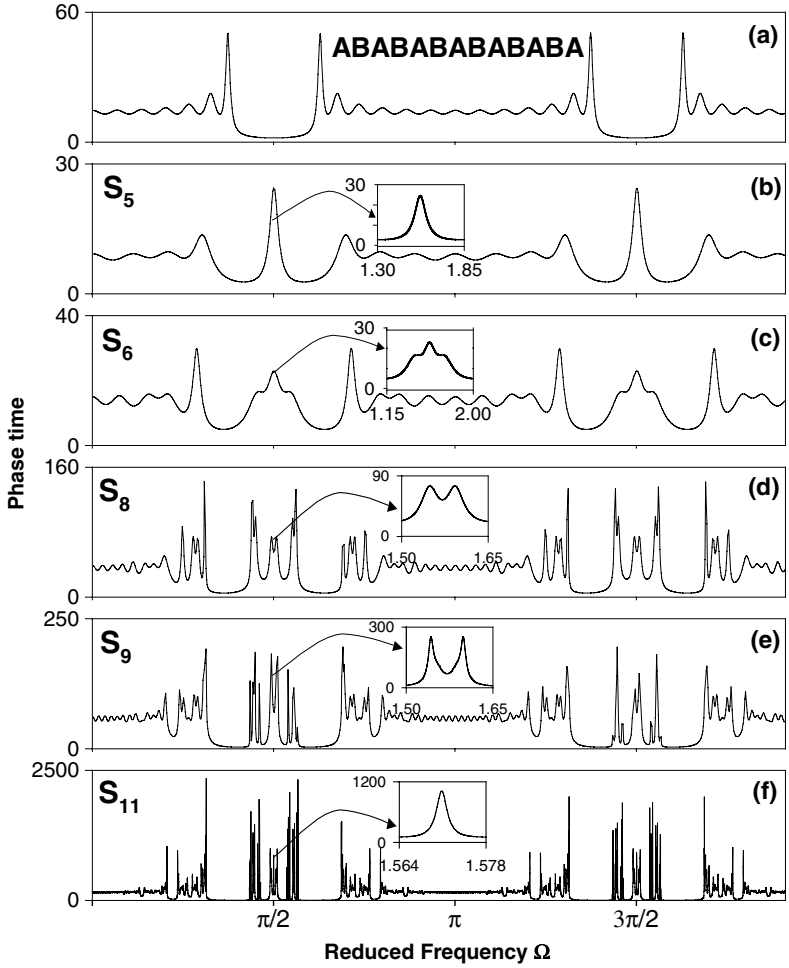

Figure 8. The same as figure 4 but the two media surrounding the structure are such that $a_s = a_B$.

there is a significant difference between the behaviours of the modes lying inside the gaps of these two structures. One can notice that the transmission (figure 7) and the phase time (figure 8), sketched for different generations, present self-similarities for a periodicity of six instead of three and for a scaling factor $f^2 \approx 41$ instead of f (see the insets of figures 7(b) and (f) and 8(b) and (f)). We have also found similar results in the case where the medium from which the incident wave is launched is of type A and the medium where the wave is transmitted is of type B and vice versa. These results are in agreement with those found theoretically by other authors [41, 47] on optical multilayered media by using the transfer matrix method and the complex effective wavenumber.

3.2. Case of asymmetric FSLS

Recently [20], some of the authors have studied stopping and filtering waves in asymmetric periodic serial loop structures. In what follows, we address the problem of an asymmetric FSLS where the lengths of the two arms constituting the loops are different. In particular,

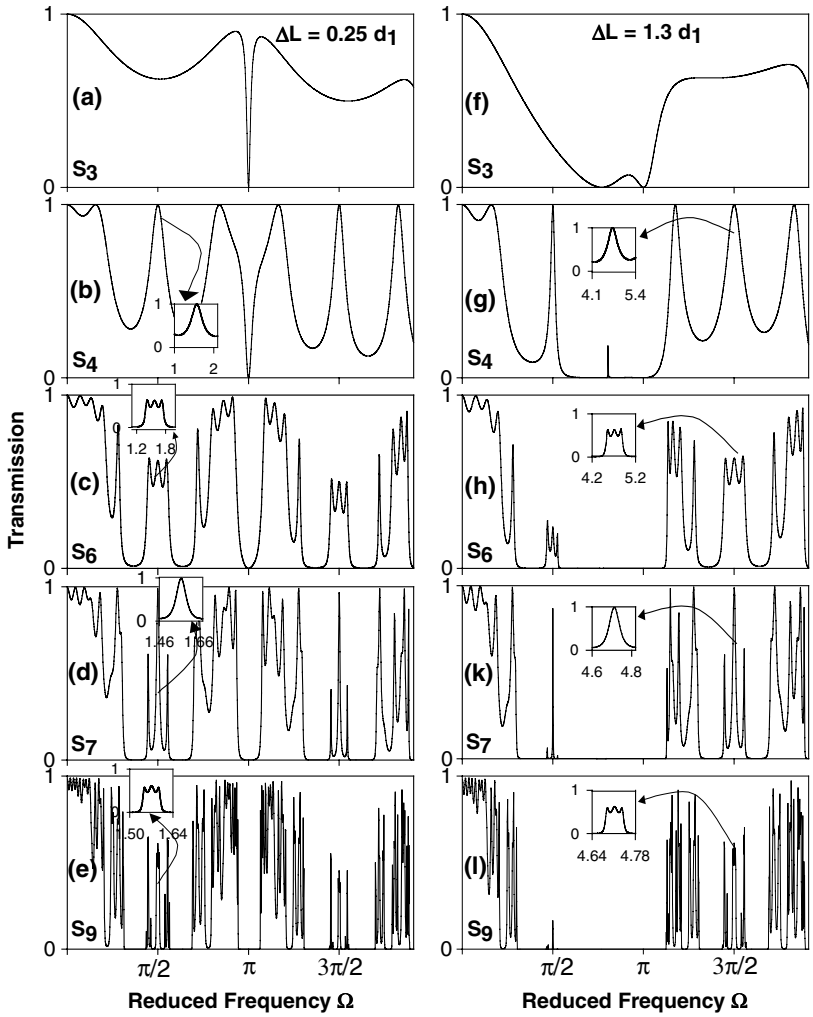

Figure 9. The same as figure 2 but for an asymmetric Fibonacci serial loop structure such that $\Delta L = 0.25d_1$ (left panel) and $\Delta L = 1.3d_1$ (right panel).

we suppose that the total length of the loop $L = d_2 + d_3$ is kept constant and equal to $2d_1$, while the difference $\Delta L = d_2 - d_3$ between the lengths of both tubes inside the loop is a varying parameter. Figure 9 gives the transmission as a function of the reduced frequency Ω for $\Delta L = 0.25d_1$ (left panel) and $\Delta L = 1.3d_1$ (right panel) respectively. Figures 9(a) and (f) clearly show successive minima in the transmission amplitude for the third generation (S_3). These minima are introduced by the asymmetric loop sandwiched between two semi-infinite slender tubes of type A. Their frequencies are given by [33]

$$\sin(\omega L/2v_0) = 0 \qquad \text{and} \qquad \cos(\omega \Delta L/2v_0) = 0. \tag{17}$$

For example, the transmission zeros lying at $\Omega = \pi$ in figures 9(a) and (b) are given by the former equation, which means that they are independent of ΔL; on the other hand, the transmission zero at $\Omega = 0.77\pi$ in figure 9(f) is given by the latter equation. Now, by increasing the generation numbers (figure 9), the transmission zeros enlarge into gaps giving

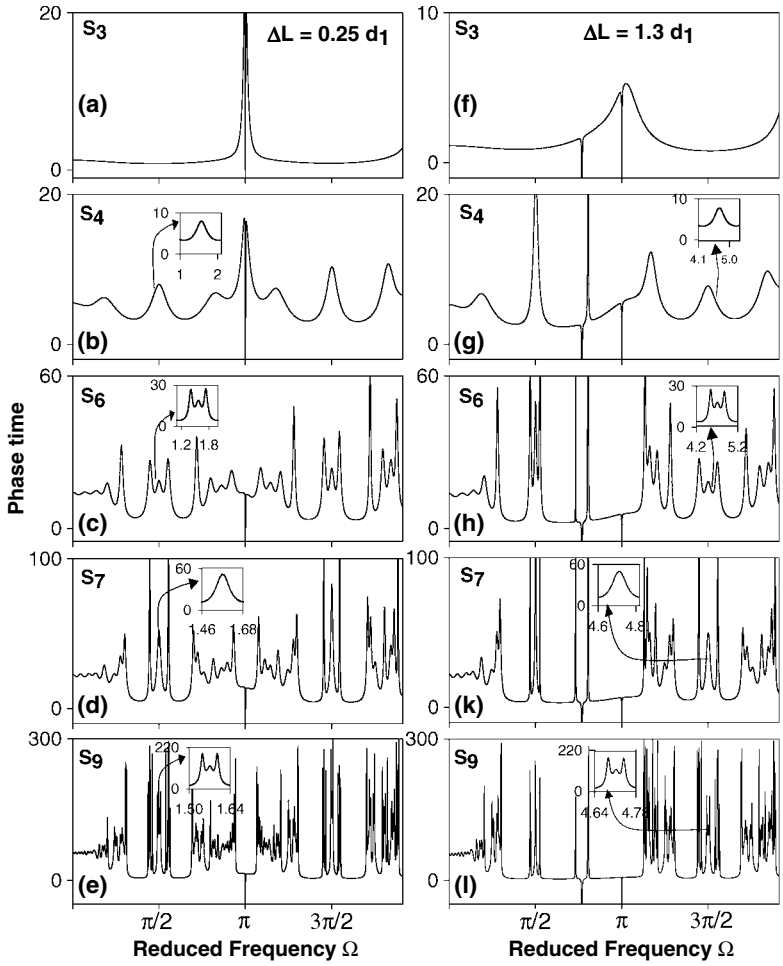

Figure 10. The same as figure 9 but for the transmission phase time.

rise to a large gap as is the case for $\Delta L = 1.3$ (figures 9(g)–(l)). At the same time other normal gaps appear which are introduced by the quasi-periodicity of the structure. One can also notice that the three-recursion scaling property still remains valid around the central frequency in the asymmetric FSLS (see for example the insets of figures 9(c) and (e)). As mentioned in section (2.3), the transmission zeros give rise to abrupt phase change by π in the phase of the transmission function or negative delta peaks in the transmission phase time as illustrated in figure 10. These results show, in accordance with section (2.3), that the phase time in asymmetric FSLS can differ from the density of states by the occurrence of additional delta peaks [33]. Also, the negative phase time may give rise to negative group velocities around the transmission zeros especially if the structures present a small absorption to enlarge the delta peaks [33]. In order to give a better insight into the effect of ΔL on the dispersion curves, we plotted in figure 11 the frequencies versus $\Delta L/d_1$ for the eighth generation. The frequencies (dots) are obtained from the maximum of the phase time. The dashed horizontal and curved lines correspond to the frequencies at which the transmission through a single asymmetric loop is equal to zero (see equation (17)). In the particular case where $\Delta L = 0$ (i.e. $d_2 = d_3$) the asymmetric FSLS becomes symmetric and therefore the gaps around $\Omega = 1.2, 2, 4.3$ and 5.1

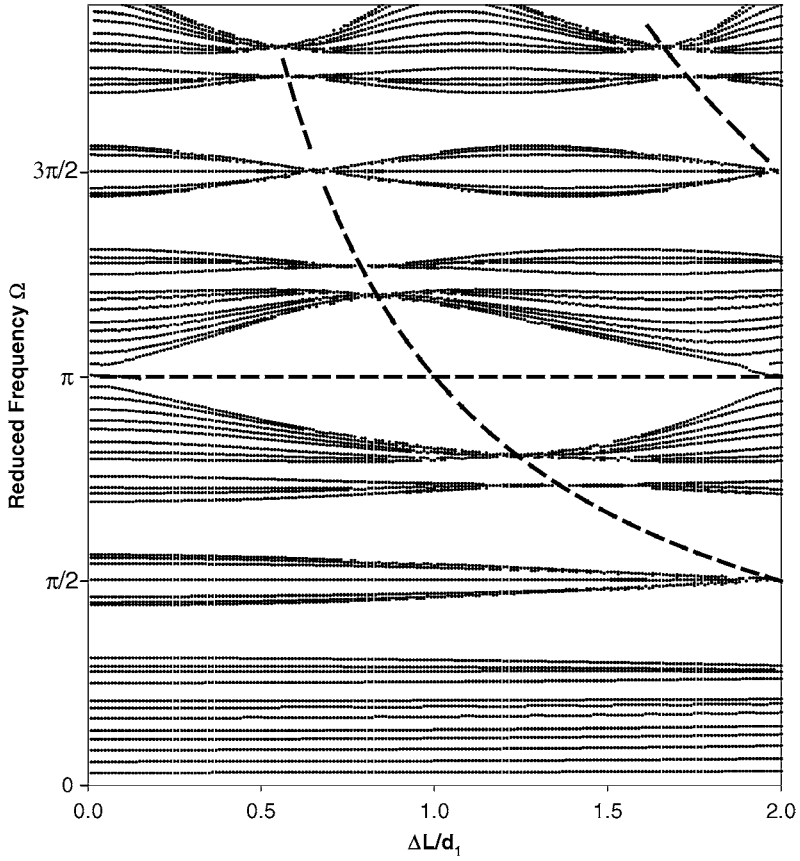

Figure 11. The projected band structure of the eighth Fibonacci generation (reduced frequency Ω as a function of $\Delta L = d_2 - d_3$ for $L = d_2 + d_3 = 2d_1$). The dots are obtained from the maxima of the transmission phase time. The dashed curves indicate the frequencies at which the transmission through a single asymmetric loop vanishes.

are introduced by the periodicity of the structure. These stop bands are not dependent on the variation of ΔL. However, when ΔL increases, some new gaps of lozenge pattern appear at the crossings of the horizontal and curved dashed lines. These gaps are the consequences of the transmission zeros induced by the asymmetric loops (figures 9 and 10), which play the role of resonators. There are also some secondary narrow minigaps along the dashed curved lines. For $\Delta L = 2d_1$ (i.e., $d_2 = 2d_1$ and $d_3 = 0$), called tangent loops [33], one can show that each loop is equivalent to two dangling side branches of lengths $d_2/2 = d_1$. It is worth noticing that the gaps induced by the transmission zeros are without analogue in the case of layered media [48].

4. Summary and conclusions

In this paper, we have presented theoretical evidence for the localization of acoustic waves in waveguide structures made of slender loop tubes pasted together by slender tubes following the Fibonacci sequence. In the case of symmetric loops, the FSLS may play the role of a simple diameter-modulated tube, which enables us to check easily different localization properties of

Fibonacci 1D layered-like media. In particular, we have shown that the Fibonacci transmission scaling property holds for a periodicity of three or six depending on the nature of the substrates surrounding the finite structure. An analysis of the local density of states clearly shows the spatial localization of the different modes propagating through the FSLS. When the loops are asymmetrical, the latter play the role of resonators that may introduce transmission zeros and hence new gaps unnoticed in the case of layered media. A study of the phase of the transmission function enables us to deduce several properties on the wave propagation through such structures as the dispersion curves, the phase times and therefore the density of states as well as the group velocities. In particular, the three- and six-cyclic Fibonacci scalings are also shown to be valid for the phase time and the group velocity. In addition, we have shown that the propagation of acoustic waves in FSLS may give rise to unusual (strong normal) dispersion inside the gaps yielding fast (slow) group velocities. We hope that these findings can be verified in an easily realizable set of experiments [13, 18, 19]. Such systems can find some useful applications in the designing of transducers and acoustic filters.

As a final remark, let us emphasize that the calculations presented here for the acoustic waves can be transposed straightforwardly to the propagation of electromagnetic waves in an FSLS when each constituent is characterized by a local dielectric constant $\epsilon(\omega)$ and an electromagnetic impedance. This is because both the equations of motion and the boundary conditions in the above problems involve similar mathematical equations [33]. Therefore, the general behaviour and conclusions obtained in this paper will prove to be useful for the electromagnetic physical problem [49]. Indeed, the loop in block B of the FSLS acts similarly to a Mach–Zehnder interferometer in optics. Our model is also valid for other quasiperiodic structures such as Thue–Morse, Rudin–Shapiro and double-period systems [21].

Acknowledgments

EEB gratefully acknowledges the hospitality of the Laboratoire de Dynamique et Structures des Matériaux Moléculaires, University de Lille 1. The work of VRV has been partially supported by the Ministerio de Ciencia y Tecnología (Spain) through grant MAT2003-04278.

References

[1] Yablonovitch E 1987 *Phys. Rev. Lett.* **58** 2059
[2] John S 1987 *Phys. Rev. Lett.* **58** 2486
[3] Soukoulis C M 1993 *Photonic Band Gaps Localization* (New York: Plenum)
[4] Joannopoulous J D, Meade R D and Winn J N 1995 *Photonic Crystals* (Princeton, NJ: Princeton University Press)
[5] Kushwaha M S, Halevi P, Dobrzynski L and Djafari-Rouhani B 1993 *Phys. Rev. Lett.* **71** 2022
Sigalas M and Economou E N 1993 *Solid State Commun.* **86** 141
Psaroba I E and Sigalas M M 2002 *Phys. Rev.* B **66** 052301
Sainidou R, Stefanou N, Psarobas I E and Modinos A 2002 *Phys. Rev.* B **66** 024303
[6] Montero de Espinoza F R, Jimnez E and Torres M 1998 *Phys. Rev. Lett.* **80** 1208
Vasseur J O, Deymier P A, Frantziskonis G, Hong G and Djafari-Rouhani B 1998 *J. Phys.: Condens. Matter* **10** 6051
Liu Z, Zhang X, Mao Y, Zhu Y Y, Yang Z, Chan C T and Sheng P 2000 *Science* **289** 1734
Yang S, Page J H, Liu Z, Cowan M L, Chan C T and Sheng P 2002 *Phys. Rev. Lett.* **88** 104301
Robertson W M and Rudy J F III 1998 *J. Acoust. Soc. Am.* **104** 694
[7] Narayanamurti V 1981 *Science* **213** 717
[8] Sagami K, Gen H, Morimoto M and Takahashi D 1996 *Acoustica* **82** 45
[9] Sheng S D, Zhu Y Y, Lu Y L and Ming N B 1995 *Appl. Phys. Lett.* **66** 291
[10] Bria D and Djafari-Rouhani B 2002 *Phys. Rev.* E **66** 056609 and references therein

[11] Manzanarez-Martinez B, Sanchez-Dehesa J, Hakansson A, Cervera F and Ramos-Mendieta F 2004 *Appl. Phys. Lett.* **85** 154
[12] Bradley C E 1994 *J. Acoust. Soc. Am.* **96** 1844
Bradley C E 1995 *J. Acoust. Soc. Am.* **188** 717
Bradley C E 1996 *J. Acoust. Soc. Am.* **100** 304
[13] Bradley C E 1994 *J. Acoust. Soc. Am.* **96** 1854
[14] Kushwaha M S, Akjouj A, Djafari-Rouhani B, Dobrzynski L and Vasseur J O 1998 *Solid State Commun.* **106** 659
[15] Wang X F, Kushwaha M S and Vasilopoulos P 2001 *Phys. Rev.* B **65** 035107
[16] Carr C and Yu R 2002 *Am. J. Phys.* **70** 1154
[17] Robertson W M, Ash J and McGaugh J M 2002 *Am. J. Phys.* **70** 689
[18] Munday J N, Brad Bennett C and Robertson W M 2002 *J. Acoust. Soc. Am.* **112** 1353
[19] Robertson W M, Baker C and Brad Bennett C 2004 *Am. J. Phys.* **72** 255
[20] Akjouj A, Al-Wahsh H, Sylla B, Djafari-Rouhani B and Dobrzynski L 2004 *J. Phys.: Condens. Matter* **16** 37
[21] For a recent review, see for example, Albuquerque E L and Cottam M G 2003 *Phys. Rep.* **376** 225
[22] Merlin R, Bajema K and Clarke R 1985 *Phys. Rev. Lett.* **55** 1768
[23] Bajema K and Merlin R 1987 *Phys. Rev.* B **36** 4555
[24] Hurley D C, Tamura S, Wolfe J P, Ploog K and Nagle J 1988 *Phys. Rev.* B **37** 8829
[25] Macia E and Dominguez-Adame F 2000 *Electrons, Phonons and Excitons in Low Dimensional Aperiodic Systems* (Madrid: Editorial Complutense)
[26] Perez-Alvarez R and García-Moliner F 2001 *Some Contemporary Problems of Condensed Matter Physics* ed S J Vlaev and L M Gaggero-Sager (New York: Nova-Science) pp 1–37
[27] Weaver R L 1990 *Wave Motion* **12** 129
Weaver R L 1993 *Phys. Rev.* B **47** 1077
[28] Smith D T, Lorenson C P and Hallock R B 1989 *Phys. Rev.* B **40** 6634
[29] He S and Maynard J D 1986 *Phys. Rev. Lett.* **57** 3171
[30] Macon L, Desideri J P and Sornette D 1991 *Phys. Rev.* B **44** 6755
[31] Gellermann W, Kohmoto M, Sutherland B and Taylor P C 1994 *Phys. Rev. Lett.* **72** 633 and references therein
[32] Dobrzynski L 1990 *Surf. Sci. Rep.* **11** 139
[33] Vasseur J O, Akjouj A, Dobrzynski L, Djafari-Rouhani B and El Boudouti E H 2004 *Surf. Sci. Rep.* **54** 1
[34] Buttiker M and Landauer R 1982 *Phys. Rev. Lett.* **49** 1739
Hauge E H and Stoveng J A 1989 *Rev. Mod. Phys.* **61** 917
[35] Lahlaouti M L H, Akjouj A, Djafari-Rouhani B, Dobrzynski L, Hammouchi M, El Boudouti E H, Nougaoui A and Kharbouch B 2001 *Phys. Rev.* B **63** 035312
[36] Taniguchi T and Buttiker M 1999 *Phys. Rev.* B **60** 13814
Lee H-W 1999 *Phys. Rev. Lett.* **82** 2358
[37] Kohmoto M, Sutherland B and Iguchi K 1987 *Phys. Rev. Lett.* **58** 2436
[38] Macia E and Dominguez-Adame F 1996 *Phys. Rev. Lett.* **76** 2957
[39] Fujiwara T, Kohmoto M and Tokihiro T 1989 *Phys. Rev.* B **40** 7413
Soukoulis C M and Economou E N 1982 *Phys. Rev. Lett.* **48** 1043
[40] Ryu C S, Oh G Y and Lee M H 1992 *Phys. Rev.* B **46** 5162
Ryu C S, Oh G Y and Lee M H 1993 *Phys. Rev.* B **48** 132
[41] Vasconcelos M S, Albuquerque E L and Mariz A M 1998 *J. Phys.: Condens. Matter* **10** 5839
[42] Kohmoto M, Sutherland B and Tang C 1987 *Phys. Rev.* B **35** 1020
Kohmoto M and Banvar J R 1986 *Phys. Rev.* B **34** 563
[43] Scalora M, Flynn R J, Reinhardt S B, Fork R L, Bloemer M J, Tocci M D, Bowden C M, Ledbetter H S, Bendickson J M and Dowling J P 1996 *Phys. Rev.* E **54** R1078
[44] Dal Negro L, Oton C J, Gaburro Z, Pavesi L, Johnson P, Lagendijk A, Righini R, Colocci M and Wiersma D S 2003 *Phys. Rev. Lett.* **90** 055501
[45] Jin D and Jin G 2005 *Phys. Rev.* B **71** 014212
[46] Zhu J N, Liu N, Zheng H and Chen H 2000 *Opt. Commun.* B **174** 139
[47] Polster R, Gasparian V and Nimtz G 1997 *Phys. Rev.* E **55** 7645
[48] Aynaou H, Velasco V R, Nougaoui A, El Boudouti E H, Djafari-Rouhani B and Bria D 2003 *Surf. Sci.* **538** 101
[49] Aynaou H, El Boudouti E H, El Hassouani Y, Akjouj A, Djafari-Rouhani B, Benomar A and Velasco V 2005 *Phys. Rev.* E submitted